

PAPER • OPEN ACCESS

## Thermal noise in electro-optic devices at cryogenic temperatures

To cite this article: Sonia Mobassem *et al* 2021 *Quantum Sci. Technol.* **6** 045005

View the [article online](#) for updates and enhancements.



**IOP | ebooks™**

Bringing together innovative digital publishing with leading authors from the global scientific community.

Start exploring the collection—download the first chapter of every title for free.

# Quantum Science and Technology



PAPER

## Thermal noise in electro-optic devices at cryogenic temperatures

OPEN ACCESS

RECEIVED  
9 September 2020REVISED  
18 June 2021ACCEPTED FOR PUBLICATION  
28 June 2021PUBLISHED  
15 July 2021

Original content from this work may be used under the terms of the [Creative Commons Attribution 4.0 licence](https://creativecommons.org/licenses/by/4.0/).

Any further distribution of this work must maintain attribution to the author(s) and the title of the work, journal citation and DOI.



Sonia Mobassem<sup>1,2</sup> , Nicholas J Lambert<sup>1,2,\*</sup> , Alfredo Rueda<sup>1,2,3</sup> ,  
Johannes M Fink<sup>3</sup> , Gerd Leuchs<sup>1,2,4,5</sup>  and Harald G L Schwefel<sup>1,2,4</sup> 

<sup>1</sup> The Dodd-Walls Centre for Photonic and Quantum Technologies, New Zealand

<sup>2</sup> Department of Physics, University of Otago, New Zealand

<sup>3</sup> Institute of Science and Technology Austria, Klosterneuburg, Austria

<sup>4</sup> Max Planck Institute for the Science of Light, Erlangen, Germany

<sup>5</sup> Institute of Applied Physics of the Russian Academy of Sciences, Nizhny Novgorod, Russia

\* Author to whom any correspondence should be addressed.

E-mail: [nicholas.lambert@otago.ac.nz](mailto:nicholas.lambert@otago.ac.nz) and [harald.schwefel@mpl.mpg.de](mailto:harald.schwefel@mpl.mpg.de)

**Keywords:** electro-optic, up-conversion, thermal noise, quantum technologies

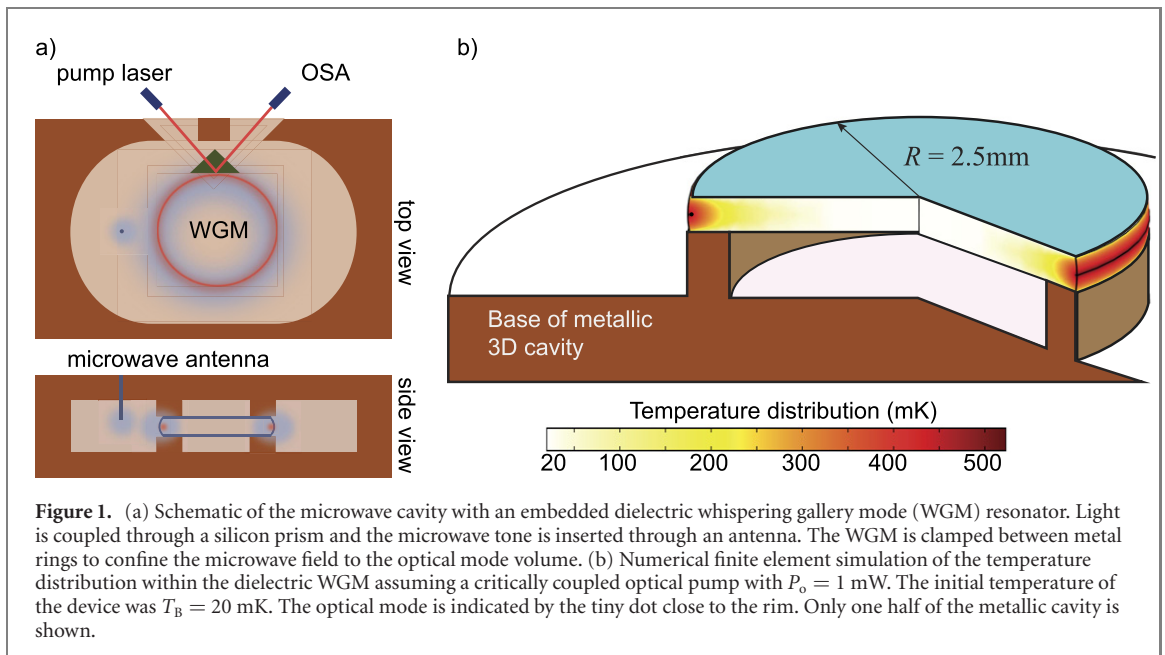
### Abstract

The quantum bits (qubits) on which superconducting quantum computers are based have energy scales corresponding to photons with GHz frequencies. The energy of photons in the gigahertz domain is too low to allow transmission through the noisy room-temperature environment, where the signal would be lost in thermal noise. Optical photons, on the other hand, have much higher energies, and signals can be detected using highly efficient single-photon detectors. Transduction from microwave to optical frequencies is therefore a potential enabling technology for quantum devices. However, in such a device the optical pump can be a source of thermal noise and thus degrade the fidelity; the similarity of input microwave state to the output optical state. In order to investigate the magnitude of this effect we model the sub-Kelvin thermal behavior of an electro-optic transducer based on a lithium niobate whispering gallery mode resonator. We find that there is an optimum power level for a continuous pump, whilst pulsed operation of the pump increases the fidelity of the conversion.

## 1. Introduction

Quantum computers based on superconducting qubits [1] have seen enormous progress in recent years. Quantum coherence is preserved as a consequence of reduced dissipation and the absence of thermal photons, but this typically requires cooling to below 100 mK for qubits with characteristic frequencies of  $\sim 10$  GHz [2]. Communication between spatially separated qubits therefore presents a particular difficulty. Outside the cryogenic environment, at room temperature, the microwave frequency photons carrying the quantum information are completely swamped by thermal photons; however, visible or near infrared photons are of much higher energy and are known to be able to carry quantum information over long distances at room temperature. Therefore, a future quantum network [3, 4] will need a method of up- and down-converting microwave photons to near infrared or visible frequency photons, to enable coherent communication between different quantum systems [5–7].

A number of approaches to microwave up-conversion have been explored [8–11], using the non-linearities offered by magneto-optic materials [12–16], cold atom clouds [17–20], quantum dots [21, 22] and opto-mechanical devices [23–26]. The effect of this non-linearity is often increased by resonant enhancement of one or more of the input field, output field and optical pump. Here we focus on an electro-optic architecture [27–34], in which the required non-linearity is provided by the electro-optic tensor of lithium niobate ( $\text{LiNbO}_3$ ) [35, 36]. The input field mode is defined by a metallic microwave cavity, and the output and pump by whispering gallery modes (WGMs) [37] confined to the perimeter of a  $\text{LiNbO}_3$  disc.



The optical pump is a feature common to all up-conversion techniques, providing both the energy for the up-converted photon, and a reference frequency. The efficiency of the up-conversion process is typically improved by increasing the power in the pump, which may be as high as 1.48 mW [36], or even 6.3 mW [32] in an electro-optic realization. However, in these experiments almost all of the optical pump is dissipated, and this can conflict with the cryogenic requirements for the environment in which superconducting qubits must be hosted. Dilution fridges, which are the usual method of attaining millikelvin temperatures, have cooling powers not significantly exceeding 1 mW [38, 39] at 100 mK with around 400  $\mu$ W being more typical. Higher dissipated powers result in a dynamical thermal equilibrium with elevated temperatures. A balance exists, therefore, between choosing a pump power large enough for the up-conversion efficiency to be useful, but not so large that heating produces a high enough thermal photon population that the quality of the quantum state transfer is compromised.

The quality of the state transfer is characterized by the fidelity, which is defined as the overlap between the input and output quantum states; a fidelity of 1 corresponds to equal states (perfect conversion), and 0 to orthogonal states. Long distance quantum telecommunication [40], remote quantum state preparation [41, 42] and quantum state coherent computing [43] are often based on continuous variable (CV) states, and therefore, the fidelity between two such states lies on a continuum between 0 and 1. Examples include states of the type  $|\psi_c\rangle = (|\alpha\rangle \pm |-\alpha\rangle)/\sqrt{2}$  (so-called ‘cat’ states), which are commonly used as CV-qubits [43], and squeezed states such as  $|\psi_s\rangle = |\alpha, r\rangle$ , which are useful in telecommunication schemes [40, 44].

Up-conversion of thermal noise to the optical channel results in a reduced fidelity of state transfer. However, so does a low conversion efficiency. In order to investigate this compromise further, we carried out thermal simulations of an efficient electro-optic modulator consisting of an optical resonator coupled to a microwave cavity [35, 36, 45]. The optical resonator is a WGM resonator made of monocrystalline LiNbO<sub>3</sub>, into which light is coupled using a silicon prism (see figure 1(a)). The convex geometry of the WGM resonator and transparency of LiNbO<sub>3</sub> confine light in the rim of the resonator via total internal reflection (see figure 1(b)). The confinement of the optical mode in a very small mode volume increases the intensity of the optical field and enhances the nonlinear interaction of light in the LiNbO<sub>3</sub>. The WGM resonator is embedded in a 3D copper microwave cavity, and the geometry of both resonators maximize the overlap between microwave field and optical mode.

In order to study the effect of absorption-induced heating on our electro-optic device we numerically model heat transport in a representative geometry comprising a LiNbO<sub>3</sub> WGM resonator with major radius  $R = 2.5$  mm and side curvature  $R_c = 1.45$  mm, embedded in a copper cavity (figure 1). The heat transfer partial differential equations are solved using COMSOL Multiphysics software, which implements a finite element method combined with a stiff ordinary differential equation solver [46, 47].

Experimental values for the thermal conductivity and heat capacity of LiNbO<sub>3</sub> are only available down to 4 K and for copper to around 1 K [48–51]. The thermal conductivity and specific heat capacity of dielectrics such as LiNbO<sub>3</sub> have a  $T^3$  dependence at cryogenic temperature. On the other hand, at very low temperatures the thermal conductivity of copper is proportional to the temperature. To estimate thermal

**Table 1.** Extrapolated thermal characteristics of LiNbO<sub>3</sub> and copper with residual resistance ratio RRR = 100 (thermal conductivity) and RRR = 30 (heat capacity) at temperatures below 1 K, assuming the functional behaviour given in reference [48].

	Thermal conductivity (W m <sup>-1</sup> K <sup>-1</sup> )	Heat capacity (J kg <sup>-1</sup> K <sup>-1</sup> )	Reference
LiNbO <sub>3</sub>	$4 \cdot T^3$	$2.705 \times 10^{-4} \cdot T^3$	[49]
Cu	$500 \cdot T$	$0.01 \cdot T$	[50]

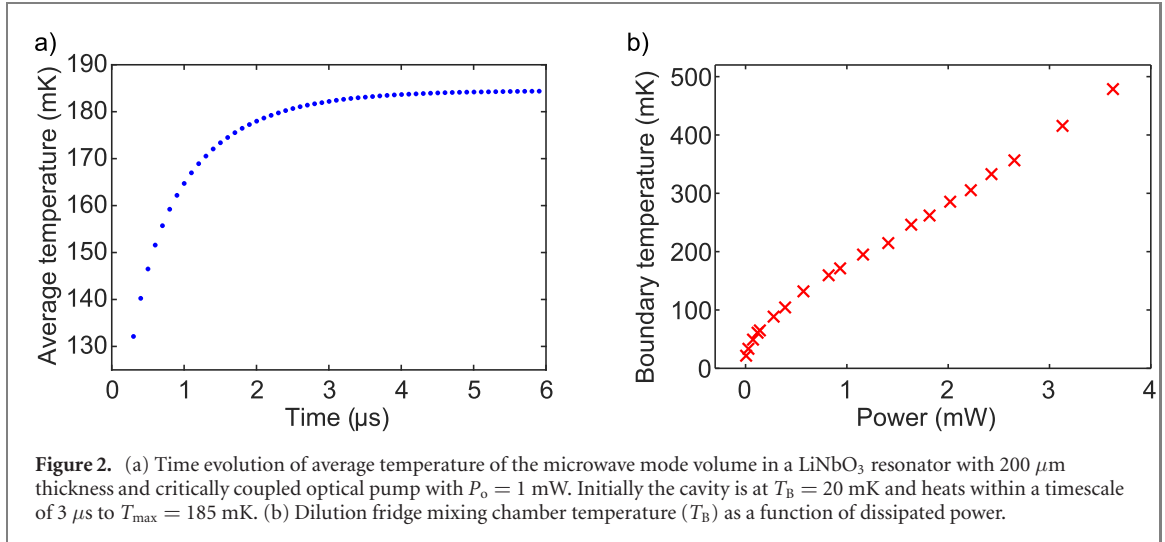


**Figure 2.** (a) Time evolution of average temperature of the microwave mode volume in a LiNbO<sub>3</sub> resonator with 200 μm thickness and critically coupled optical pump with  $P_o = 1$  mW. Initially the cavity is at  $T_B = 20$  mK and heats within a timescale of 3 μs to  $T_{max} = 185$  mK. (b) Dilution fridge mixing chamber temperature ( $T_B$ ) as a function of dissipated power.

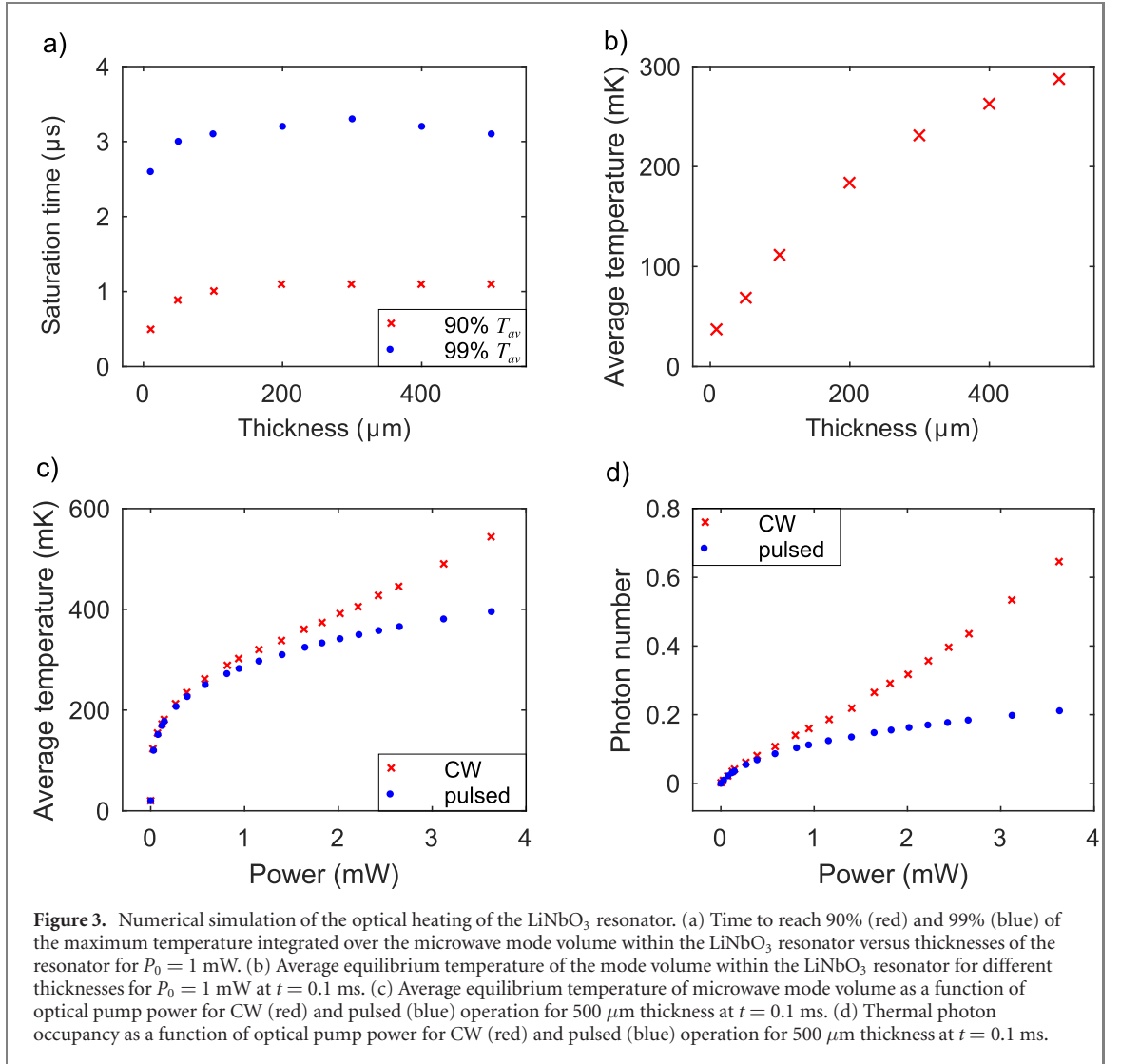
conductivity and specific heat capacity of the materials, we make appropriate downwards extrapolations from data above 4 K, as detailed in table 1. We neglect the thermal contact resistance at the LiNbO<sub>3</sub>–Cu interface, due to the smoothness of the LiNbO<sub>3</sub> and the softness of the copper generally giving a good interface, and the low thermal conductivity of the dielectric dominating heat transport (see table 1).

In the heat transfer simulation of our microwave to optical converter, the optical pump is modelled as a heat source occupying the same volume as the optical mode. The dissipated power follows an exponential approach to the pump power  $P_o$  as  $P = P_o(1 - \exp(-t/\tau))$ , where  $\tau$  is the rise time of optical mode (for our optical resonator  $\tau \sim 1$  μs, corresponding to a quality factor of  $Q \sim 10^8$ ). The thermal boundary conditions are given by the temperature of the mixing chamber plate of the fridge. As the fridge cooling power at  $T \sim 100$  mK is comparable to the heat load introduced by the optical pump, the boundary temperature  $T_B$  for CW operation is also a function of the power dissipated in our device. We determine typical mixing chamber temperatures for different heat loads by putting a known load on a resistive heater mounted at the mixing chamber of our BlueFors LD250, and then waiting for the temperature to stabilize (see figure 2(b)). The precise details of this dependency will vary between cryogenic technologies and environments.

For pulsed operation of the optical pump, the average heat load will be decreased by the duty cycle of the pump; for example, if the pump is on for only 1% of the operation cycle, then the heat load will be 1% of the pulsed power. A upper limit on the time scale for the operation of current quantum systems is the lifetime of superconducting qubits (1 ms [52]). For optical pulses of this length the temperature of the cryogenic environment will stay stable and close to its base temperature, as the thermal response time scales of the fridge are of the order of seconds. To study this mode of operation, we fix our thermal boundary around the base temperature at  $T_B = 20$  mK.

We expect the optical rise time, and therefore heating, of the device to be orders of magnitude slower than the diffusion of the heat within the dielectric. By considering the lowest order component of solutions to the heat diffusion equation, we find  $t \sim \rho C d^2 / K$ , with heat capacity  $C$ , thermal conductivity  $K$  and density  $\rho$ . For LiNbO<sub>3</sub> with a thickness of  $2d = 200$  μm, the characteristic time for the heat to be redistributed is  $t = 3$  ns.

The evolution of the temperature in the LiNbO<sub>3</sub>, considering the full geometry, is calculated as a function of time, with the LiNbO<sub>3</sub> temperature at  $t = 0$  set to the same temperature as the mixing chamber  $T_B = 20$  mK. In figure 2(a) we plot the average temperature  $T_{av}$  of LiNbO<sub>3</sub> integrated over the microwave mode volume within the dielectric as a function of time for a WGM resonator thickness of 200 μm and a pump power of 1 mW. The heating occurs on a timescales of  $\sim 3$  μs for the parameters of our cavity. We compare this calculation for the case where the optical power immediately reaches its maximum within the



optical mode volume. Here the temperature saturates after only  $\sim 6$  ns, corresponding well to the analytical toy model above.

One of the parameters affecting the time evolution of temperature is the thickness of the LiNbO<sub>3</sub> resonator, which is often reduced in order to increase the strength of the electric field across it. In figures 3(a) and (b) we show the saturation time and the asymptotic average temperature as a function of thickness. Since LiNbO<sub>3</sub> has a very low thermal conductivity compared to copper, an increase in thickness corresponds to an increase in average temperature, as well as an increase in the time taken to reach that temperature.

We now fix the thickness of the resonator at 500  $\mu\text{m}$ , and study the equilibrium thermal occupancy of the microwave cavity as a function of pump power. For a mode of temperature  $T$  and angular frequency  $\omega$ , the thermal photon number occupancy is

$$n = \frac{1}{\exp\left(\frac{\hbar\omega}{k_B T}\right) - 1}. \quad (1)$$

The total thermal photon number of the mode is given by

$$\bar{n}_\Omega = \frac{\kappa_i}{\kappa} n_{\text{th},i} + \sum_j \frac{\kappa_{e,j}}{\kappa} n_{\text{th},j}. \quad (2)$$

Here  $n_{\text{th},j}$  is the thermal occupancy of the  $j$ th port of the cavity.  $\kappa = \kappa_i + \sum_j \kappa_{e,j}$  is the total intensity loss rate of the cavity and is the sum of the internal loss rate,  $\kappa_i$ , and the loss rate via the  $j$ th port  $\kappa_{e,j}$  [8].  $n_{\text{th},i}$  is the thermal occupancy of the mode due to internal fluctuations. This is directly related to internal losses by the fluctuation–dissipation theorem [53]. Because of the large loss tangent of LiNbO<sub>3</sub>, dielectric losses are

the dominant contribution to  $\kappa_i$ . The microwave electric field within the LiNbO<sub>3</sub> is uniform, and so we use the spatial average of the temperature within the microwave mode volume inside the dielectric (figure 3(c)), as calculated for the asymptotic temperature distribution.

We calculate thermal photon numbers for the microwave mode of our single port cavity with angular frequency  $\Omega = 2\pi \times 10$  GHz as a function of pump power, while fixing the coupling rate of the port to critical coupling ( $\kappa = \kappa_i + \kappa_{e,1}$ ,  $\kappa_i = \kappa_{e,1}$ ). In figure 3(d) we present data for two possibilities, one in which the port temperature rises with increasing pump power due to the elevated mixing chamber temperature (CW operation of the optical pump) and one in which the port temperature remains constant at 20 mK (pulsed operation of the pump).

We calculate the effect of the simulated thermal noise on the fidelity of converted states using input–output theory from reference [55] for feasible experimental parameters [35]. We use the multi-photon cooperativity  $C = \frac{4n_p g^2}{\kappa_o \kappa_\Omega}$ , where  $\kappa_o(\Omega) = \kappa_{i,o(\Omega)} + \kappa_{e,o(\Omega)}$  is the total loss rate of the optical (microwave) mode, with  $\kappa_{i,o(\Omega)}$  and  $\kappa_{e,o(\Omega)}$  being the intrinsic and the extrinsic damping rates of the optical (microwave) modes, respectively. We calculate the fidelity of the system where the optical mode is overcoupled,  $\kappa_{e,o} = 4 \times \kappa_{i,o} = 2\pi \times 2.8$  MHz, and the microwave mode is critically coupled,  $\kappa_{e,\Omega} = \kappa_{i,\Omega} = 2\pi \times 32.4$  MHz.  $n_p = \frac{4\eta_o P_o}{\kappa_o \hbar\omega_p}$  is the photon number corresponding to optical pump power  $P_o$ ,  $g$  is the coupling strength and for our system  $g = 2\pi \times 7.4$  Hz. Here,  $\eta_{\Omega(o)} = \frac{\kappa_{e,\Omega(o)}}{\kappa_{\Omega(o)}}$  is the waveguide-cavity coupling.

The fidelity of the transferred coherent squeezed state  $|\alpha, r\rangle$  is given by [56]

$$F_{\text{tr}}^G(\alpha, r, C) = \frac{\exp\left(-2|\alpha|^2(\epsilon_3 - 1)^2 \left(\frac{\cos(\phi_\alpha)}{V_-} + \frac{\sin(\phi_\alpha)}{V_+}\right)\right)}{\sqrt{\frac{\epsilon_2}{2}(1 - \epsilon_3^4) + \epsilon_3^4 \left(1 + \frac{\bar{n}_\Omega(\epsilon_2 + \epsilon_2\epsilon_3^2 - 2 + \frac{\bar{n}_\Omega}{C\eta_o})}{C\eta_o}\right)}}, \quad (3)$$

where  $V_\pm = 1 + \epsilon_3^2(e^{\pm 2r} - 1 + \frac{2\bar{n}_\Omega}{\eta_o C})$ ,  $\epsilon_2 = 1 + \cosh(2r)$ ,  $\epsilon_3 = \frac{\sqrt{4\eta_o\eta_\Omega C}}{1+C}$  is the square root of the quantum conversion efficiency,  $|\alpha|$  is field amplitude,  $\phi_\alpha$  is the phase of the field, and  $\bar{n}_\Omega$  is the equilibrium mean thermal photon numbers of the microwave field equation (1). The fidelity of the transferred cat state is given by [56]

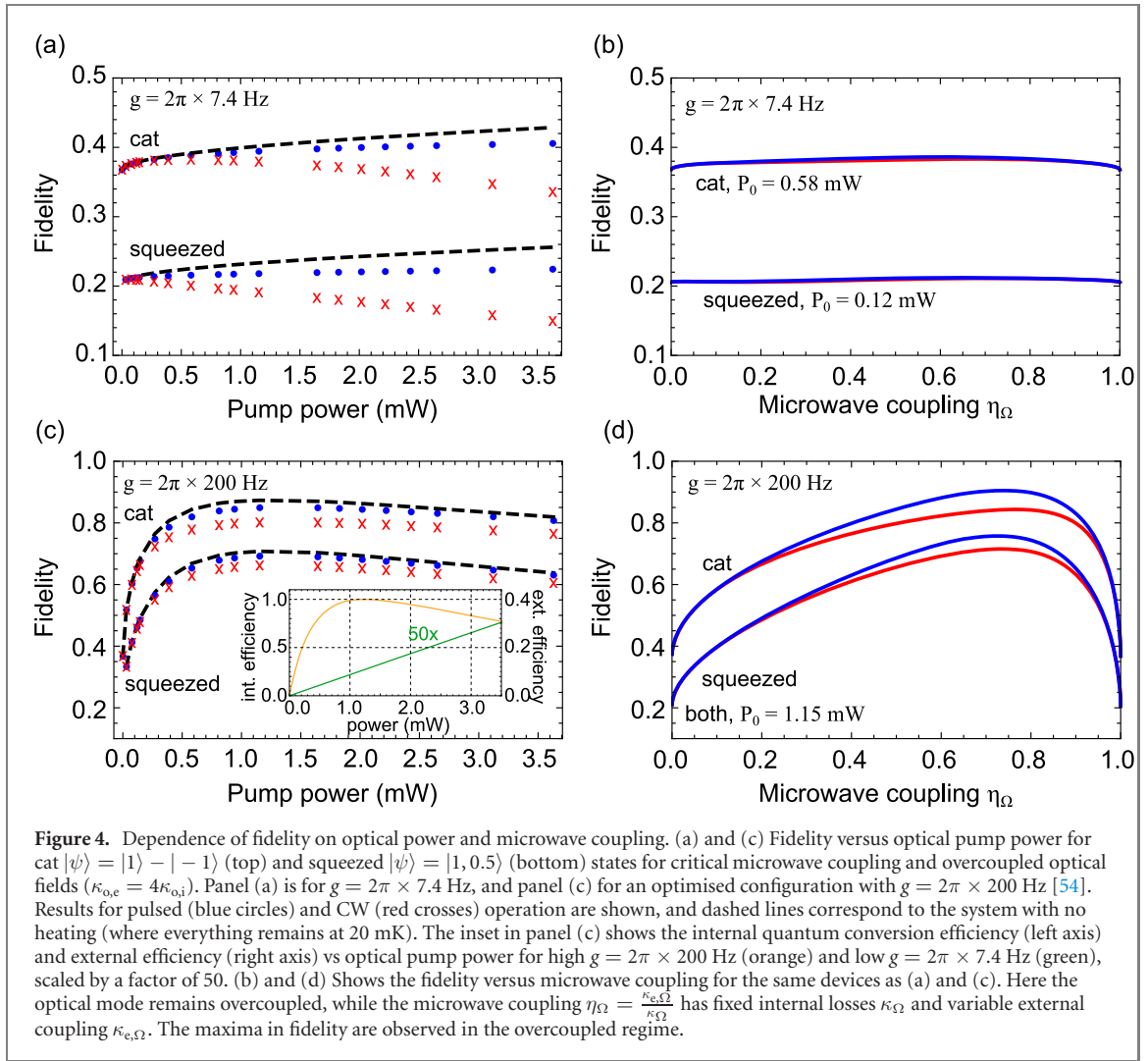
$$F_{\text{tr}}^{\text{cat}}(\alpha, C) = \frac{1}{\epsilon_4(1 + \epsilon_5)} \left[ \left(1 + e^{\frac{8\alpha^2\epsilon_3}{1+\epsilon_5}}\right) e^{-\frac{2\alpha^2(1+\epsilon_3^2)^2}{1+\epsilon_5}} + 2 \cos(\phi) \left( e^{-\frac{2\alpha^2(\epsilon_3^2+\epsilon_5)}{1+\epsilon_5}} + e^{-\frac{2\alpha^2(1+\epsilon_3^2\epsilon_5)}{1+\epsilon_5}} \right) \right. \\ \left. + \cos(2\phi) e^{-\frac{2\alpha^2(\epsilon_3+\epsilon_5)^2}{\epsilon_5(1+\epsilon_5)}} + e^{-\frac{2\alpha^2(\epsilon_3-\epsilon_5)^2}{\epsilon_5(1+\epsilon_5)}} \right], \quad (4)$$

where  $\epsilon_4 = (1 + \cos(\phi))e^{-2\alpha^2}(1 + \cos(\phi))e^{-2\alpha^2\epsilon_3^2}$  and  $\epsilon_5 = 1 + \frac{8\eta_\Omega\bar{n}_\Omega}{(1+C)^2}$ .

The fidelity for states with cooperativity  $C < 1$  [35], is shown vs the optical pump power  $P_o$  in figure 4(a), where the dashed lines show the noiseless case of a cat state  $|\psi\rangle = |1\rangle - |-1\rangle$  (top) and squeezed state  $|\psi\rangle = |1, 0.5\rangle$  (bottom). The red markers indicate CW pump operation and the blue crosses pulsed operation. The maximum fidelity for CW operation is achieved at  $P_o \approx 0.58$  mW for the cat state and  $P_o \approx 0.12$  mW for squeezed state. Fidelities for pulsed operation are shown in blue. These do not exhibit a peak, but still diverge from the fidelities for noiseless operation as the power increases. At  $P_o = 0$  the fidelity is non-zero due to the state's overlap with the vacuum.

The added noise due to dielectric heating causes a degradation of the fidelity of around 4.6% (cat state) and 4.1% (squeezed state) from the noiseless case. This problem can be reduced by over-coupling the microwave system; in this case the waveguide temperature, which is always less than the mode temperature, increases the fidelity by acting to cool the mode [36, 57, 58]. In figure 4(b), we fix the optical pump power to the maximum fidelity of figure 4(a) with  $P_o \approx 0.58$  mW for the cat state and  $P_o \approx 0.12$  mW for the squeezed state, and vary the microwave coupling from under-coupling ( $\eta_\Omega = 0$ ) to over-coupling ( $\eta_\Omega = 1$ ). For each state the red curve includes heating of the coupling waveguide (CW operation) and the blue curve describes pulsed operation which leaves the waveguide at the base temperature. We find optimal couplings for pulsed operation of  $\eta_\Omega = 0.60$  (cat state) and  $\eta_\Omega = 0.66$  (squeezed state), and for CW operation of  $\eta_\Omega = 0.61$  (cat state) and  $\eta_\Omega = 0.66$ .

We now study the effects of thermal noise on an optimised transducer. The principle route to higher efficiencies in electro-optic up-convertors is by increasing the co-operativity  $g$ . In figure 4(c) we plot fidelity as a function of pump power for a device with  $g = 2\pi \times 200$  Hz. We find that there still exists optimal pump powers. Furthermore, in figure 4(d) the maximum fidelity is found to be at higher microwave



overcouplings for pulsed operation of  $\eta_{\Omega} = 0.74$  (cat state) and  $\eta_{\Omega} = 0.78$  (squeezed state), and for CW operation of  $\eta_{\Omega} = 0.73$  (cat state) and  $\eta_{\Omega} = 0.74$ .

For quantum state conversion a maximum number of added noise photons in the output mode of 0.5 is required [59]. In electro-optic devices this corresponds to a fidelity of  $F^{\text{G}} = 0.42$ , and  $F^{\text{cat}} = 0.61$ . This is therefore a threshold necessary for useful quantum operation. To reach this threshold it is evident that besides high  $g$  careful thermal management in terms of optimal pump power and microwave coupling is paramount.

Finally, we note that in our calculations, the rise in the temperature of the copper cavity is negligible due to the relatively large heat capacity and thermal conductivity of copper, even at cryogenic temperatures. This may not be the case for superconducting cavities, in which the heat capacity is exponentially suppressed below the superconducting transition temperature. In order to consider the fidelity of conversion for discrete quantum states, such as Fock states, approximate methods such as those developed in [60] could be used. Furthermore, stray photons in a superconducting cavity may lead to a significant non-equilibrium quasiparticle population. For superconducting materials such as aluminium, an appreciable rise in the cavity material temperature may occur on longer timescales [36, 60]. Further analysis of this is beyond the scope of the present work.

In conclusion, we have demonstrated that the fidelity of quantum state transfer in electro-optic microwave-to-optical transducers is significantly affected by heating due to the absorption of the optical pump. In particular, the choice of pump power must take into account the competition between increased efficiency and increased heating that follow increased optical power. We find that, for some parameter regimes, there is an optimal power which maximises state transfer fidelity. Furthermore, there is also an optimal coupling to the microwave input waveguide which is significantly more than critical coupling. Whilst our calculations have used an electro-optic structure as an archetype, the universality of the need for an optical pump in quantum transducers means that our conclusions can be extended to other platforms. Recently optomechanical micro-devices have been demonstrated with efficient microwave-optical photon

conversion [61, 62]. However, they too suffer from large thermal noise even at millikelvin temperatures when pump power is increased over a certain limit ( $\sim 625$  pW [61],  $\sim 40$  mW [62]), showing the universal applicability of our analysis.

## Acknowledgments

NJL is supported by the MBIE Endeavour Fund (UOOX1805) and GL is by the Julius von Haast Fellowship of New Zealand. SM acknowledges stimulating discussions with T M Jensen.

## Data availability statement

The data that support the findings of this study are available upon reasonable request from the authors.

## ORCID iDs


Sonia Mobassem  <https://orcid.org/0000-0002-7648-0990>

Nicholas J Lambert  <https://orcid.org/0000-0001-5202-4838>

Alfredo Rueda  <https://orcid.org/0000-0001-6249-5860>

Johannes M Fink  <https://orcid.org/0000-0001-8112-028X>

Gerd Leuchs  <https://orcid.org/0000-0003-1967-2766>

Harald G L Schwefel  <https://orcid.org/0000-0002-4304-6469>

## References

- [1] Devoret M H and Schoelkopf R J 2013 Superconducting circuits for quantum information: an outlook *Science* **339** 1169–74
- [2] Devoret M H and Martinis J M 2004 Implementing qubits with superconducting integrated circuits *Quantum Inf. Process.* **3** 163–203
- [3] Kimble H J 2008 The quantum internet *Nature* **453** 1023–30
- [4] Wehner S, Elkouss D and Hanson R 2018 Quantum internet: a vision for the road ahead *Science* **362** eaam9288 Publisher: American Association for the Advancement of Science Section: Review
- [5] DiVincenzo D P 2000 The physical implementation of quantum computation *Fortschr. Phys.* **48** 771–83
- [6] Simon C 2017 Towards a global quantum network *Nat. Photon.* **11** 678–80
- [7] Huang J and Kumar P 1992 Observation of quantum frequency conversion *Phys. Rev. Lett.* **68** 2153–6
- [8] Lambert N J, Rueda A, Sedlmeir F and Schwefel H G L 2020 Coherent conversion between microwave and optical photons—an overview of physical implementations *Adv. Quantum Tech.* **3** 1900077
- [9] Clerk A A, Lehnert K W, Bertet P, Petta J R and Nakamura Y 2020 Hybrid quantum systems with circuit quantum electrodynamics *Nat. Phys.* **16** 257–67
- [10] Kurizki G, Bertet P, Kubo Y, Mølmer K, Petrosyan D, Rabl P and Schmiedmayer J 2015 Quantum technologies with hybrid systems *Proc. Natl Acad. Sci. USA* **112** 3866–73
- [11] Lauk N, Sinclair N, Barzanjeh S, Covey J P, Saffman M, Spiropulu M and Simon C 2020 Perspectives on quantum transduction *Quantum Sci. Technol.* **5** 020501 Publisher: IOP Publishing
- [12] Williamson L A, Chen Y-H and Longdell J J 2014 Magneto-optic modulator with unit quantum efficiency *Phys. Rev. Lett.* **113** 203601
- [13] Fernandez-Gonzalvo X, Chen Y-H, Yin C, Rogge S and Longdell J J 2015 Coherent frequency up-conversion of microwaves to the optical telecommunications band in an Er:YSO crystal *Phys. Rev. A* **92** 062313
- [14] Everts J R, Berrington M C, Ahlefeldt R L and Longdell J J 2019 Microwave to optical photon conversion via fully concentrated rare-earth-ion crystals *Phys. Rev. A* **99** 063830
- [15] Haigh J A, Nunnenkamp A, Ramsay A J and Ferguson A J 2016 Triple-resonant Brillouin light scattering in magneto-optical cavities *Phys. Rev. Lett.* **117** 133602
- [16] Hisatomi R, Osada A, Tabuchi Y, Ishikawa T, Noguchi A, Yamazaki R, Usami K and Nakamura Y 2016 Bidirectional conversion between microwave and light via ferromagnetic magnons *Phys. Rev. B* **93** 174427
- [17] Hafezi M, Kim Z, Rolston S L, Orozco L A, Lev B L and Taylor J M 2012 Atomic interface between microwave and optical photons *Phys. Rev. A* **85** 020302
- [18] Han J, Vogt T, Gross C, Jaksch D, Kiffner M and Li W 2018 Coherent microwave-to-optical conversion via six-wave mixing in Rydberg atoms *Phys. Rev. Lett.* **120** 093201
- [19] Vogt T, Gross C, Han J, Pal S B, Lam M, Kiffner M and Li W 2019 Efficient microwave-to-optical conversion using Rydberg atoms *Phys. Rev. A* **99** 023832 Publisher: American Physical Society
- [20] Zibrov A S, Matsko A B and Scully M O 2002 Four-wave mixing of optical and microwave fields *Phys. Rev. Lett.* **89** 103601
- [21] Rakher M T, Ma L, Slattery O, Tang X and Srinivasan K 2010 Quantum transduction of telecommunications-band single photons from a quantum dot by frequency upconversion *Nat. Photon.* **4** 786–91
- [22] Singh A *et al* 2019 Quantum frequency conversion of a quantum dot single-photon source on a nanophotonic chip *Optica* **6** 563–9
- [23] Andrews R W, Peterson R W, Purdy T P, Cicak K, Simmonds R W, Regal C A and Lehnert K W 2014 Bidirectional and efficient conversion between microwave and optical light *Nat. Phys.* **10** 321–6
- [24] Bagci T *et al* 2014 Optical detection of radio waves through a nanomechanical transducer *Nature* **507** 81–5



- [25] Stannigel K, Rabl P, Sørensen A S, Zoller P and Lukin M D 2010 Optomechanical transducers for long-distance quantum communication *Phys. Rev. Lett.* **105** 220501
- [26] Higginbotham A P, Burns P S, Urmey M D, Peterson R W, Kampel N S, Brubaker B M, Smith G, Lehnert K W and Regal C A 2018 Harnessing electro-optic correlations in an efficient mechanical converter *Nat. Phys.* **14** 1038
- [27] Strekalov D V, Schwefel H G L, Savchenkov A A, Matsko A B, Wang L J and Yu N 2009 Microwave whispering-gallery resonator for efficient optical up-conversion *Phys. Rev. A* **80** 033810
- [28] Tsang M 2010 Cavity quantum electro-optics *Phys. Rev. A* **81** 063837
- [29] Javerzac-Galy C, Plekhanov K, Bernier N R, Toth L D, Feofanov A K and Kippenberg T J 2016 On-chip microwave-to-optical quantum coherent converter based on a superconducting resonator coupled to an electro-optic microresonator *Phys. Rev. A* **94** 053815
- [30] Soltani M, Zhang M, Ryan C, Ribeill G J, Wang C and Loncar M 2017 Efficient quantum microwave-to-optical conversion using electro-optic nanophotonic coupled resonators *Phys. Rev. A* **96** 043808
- [31] Zhang M, Wang C, Buscaino B, Shams-Ansari A, Kahn J M and Loncar M 2018 Electro-optic frequency comb generation in ultrahigh-Q integrated lithium niobate micro-resonators *2018 Conf. on Lasers and Electro-Optics (CLEO)* pp 1–2
- [32] Fan L, Zou C-L, Cheng R, Guo X, Han X, Gong Z, Wang S and Tang H X 2018 Superconducting cavity electro-optics: a platform for coherent photon conversion between superconducting and photonic circuits *Sci. Adv.* **4** eaar4994
- [33] Witmer J D, McKenna T P, Arrangoiz-Arriola P, Van Laer R, Alex Wollack E, Lin F, Jen A K-Y, Luo J and Safavi-Naeini A H 2020 A silicon-organic hybrid platform for quantum microwave-to-optical transduction *Quantum Sci. Technol.* **5** 034004 Publisher: IOP Publishing
- [34] Rueda A 2021 Frequency-multiplexed hybrid optical entangled source based on the Pockels effect *Phys. Rev. A* **103** 023708
- [35] Rueda A et al 2016 Efficient microwave to optical photon conversion: an electro-optical realization *Optica* **3** 597
- [36] Hease W, Rueda A, Sahu R, Wulf M, Arnold G, Schwefel H G L and Fink J M 2020 Bidirectional electro-optic wavelength conversion in the quantum ground state *PRX Quantum* **1** 020315
- [37] Strekalov D V, Marquardt C, Matsko A B, Schwefel H G L and Leuchs G 2016 Nonlinear and quantum optics with whispering gallery resonators *J. Opt.* **18** 123002
- [38] Uhlig K 2008 Dry dilution refrigerator with high cooling power *AIP Conf. Proc.* **985** 1287–91
- [39] XLD Series Dilution Refrigerator (Library Catalog: bluefors.com)
- [40] Braunstein S L and Pati A K 2012 *Quantum Information with Continuous Variables* (Berlin: Springer)
- [41] Laurat J, Coudreau T, Treps N, Maitre A and Fabre C 2003 Conditional preparation of a quantum state in the continuous variable regime: generation of a sub-Poissonian state from twin beams *Phys. Rev. Lett.* **91** 213601
- [42] Pogorzalek S et al 2019 Secure quantum remote state preparation of squeezed microwave states *Nat. Commun.* **10** 1–6
- [43] Neergaard-Nielsen J S, Takeuchi M, Wakui K, Takahashi H, Hayasaka K, Takeoka M and Sasaki M 2010 Optical continuous-variable qubit *Phys. Rev. Lett.* **105** 053602
- [44] Weedbrook C, Pirandola S, García-Patrón R, Cerf N J, Ralph T C, Shapiro J H and Lloyd S 2012 Gaussian quantum information *Rev. Mod. Phys.* **84** 621–69
- [45] Rueda A, Sedlmeir F, Kumari M, Leuchs G and Schwefel H G L 2019 Resonant electro-optic frequency comb *Nature* **568** 378
- [46] COMSOL Multiphysics® v. 5.6. [www.comsol.com](http://www.comsol.com). COMSOL AB, Stockholm, Sweden COMSOL: Multiphysics software for Optimizing Designs
- [47] Edsberg L 2015 *Introduction to Computation and Modeling for Differential Equations* (New York: Wiley)
- [48] Krinner S, Storz S, Kurpiers P, Magnard P, Heinsoo J, Keller R, Lütolf J, Eichler C and Wallraff A 2019 Engineering cryogenic setups for 100-qubit scale superconducting circuit systems *EPJ Quantum Technol.* **6** 1–29
- [49] Pérez-Enciso E and Vieira S 1998 Thermal properties of intrinsically disordered LiNbO<sub>3</sub> crystals at low temperatures *Phys. Rev. B* **57** 13359–62
- [50] Duthil P 2014 Material Properties at Low Temperature 24 April - 4 May 2013 Erice, Italy *CAS-CERN Accelerator School: Superconductivity for Accelerators* ed R Bailey pp 77–95
- [51] Woodcraft A L 2005 Recommended values for the thermal conductivity of aluminium of different purities in the cryogenic to room temperature range, and a comparison with copper *Cryogenics* **45** 626–36
- [52] Kjaergaard M, Schwartz M E, Braumüller J, Krantz P, Wang J I-J, Gustavsson S and Oliver W D 2020 Superconducting qubits: current state of play *Annu. Rev. Condens. Matter Phys.* **11** 369–95 Publisher: Annual Reviews
- [53] Gardiner C and Zoller P 2004 *Quantum Noise: A Handbook of Markovian and Non-Markovian Quantum Stochastic Methods with Applications to Quantum Optics* (Berlin: Springer)
- [54] Rueda Sanchez A R 2018 Resonant Electrooptics *PhD Thesis* University of Erlangen-Nürnberg, Erlangen, Germany
- [55] Savchenkov A A, Ilchenko V S, Matsko A B and Maleki L 2003 Tunable filter based on whispering gallery modes *Electron. Lett.* **39** 389–91
- [56] Rueda A, Hease W, Barzanjeh S and Fink J M 2019 Electro-optic entanglement source for microwave to telecom quantum state transfer *npj Quantum Inf.* **5** 1–11
- [57] Santamaría Botello G et al 2018 Sensitivity limits of millimeter-wave photonic radiometers based on efficient electro-optic upconverters *Optica* **5** 1210–9
- [58] Xu M, Han X, Zou C-L, Fu W, Xu Y, Zhong C, Jiang L and Tang H X 2020 Radiative cooling of a superconducting resonator *Phys. Rev. Lett.* **124** 033602
- [59] Andrews R W, Reed A P, Cicak K, Teufel J D and Lehnert K W 2015 Quantum-enabled temporal and spectral mode conversion of microwave signals *Nat. Commun.* **6** 10021
- [60] McKenna T P, Witmer J D, Patel R N, Jiang W, Van Laer R, Arrangoiz-Arriola P, Alex Wollack E, Herrmann J F and Safavi-Naeini A H 2020 Cryogenic microwave-to-optical conversion using a triply-resonant lithium niobate on sapphire transducer *Optica* **7** 1737–45
- [61] Arnold G, Wulf M, Barzanjeh S, Redchenko E S, Rueda A, Hease W J, Hassani F and Fink J M 2020 Converting microwave and telecom photons with a silicon photonic nanomechanical interface *Nat. Commun.* **11** 4460
- [62] Han X et al 2020 Cavity piezo-mechanics for superconducting-nanophotonic quantum interface *Nat. Commun.* **11** 3237